Re-growth, morphogenesis, and differentiation during starfish arm regeneration

Yousra Ben Khadra, MS[1]; Cinzia Ferrario, MS[2]; Cristiano Di Benedetto, PhD[2,3]; Khaled Said, PhD[1]; Francesco Bonasoro, PhD[2]; M. Daniela Candia Carnevali, MS[2]; Michela Sugni, PhD[2]

1. Laboratory of Genetics, Biodiversity and Valorization of Bioresources, Higher Institute of Biotechnology, University of Monastir, Monastir, Tunisia,
2. Department of Biosciences, University of Milan, Milan, Italy,
3. Biological and Environmental Sciences and Engineering Division, King Abdullah University of Science and Technology (KAUST), 23955-6900 Thuwal, Saudi Arabia

Reprint requests:
Cinzia Ferrario, Dipartimento di Bioscienze, Università degli Studi di Milano Via Celoria 26, 20133, Milano, Italy.
Tel: +390250314799;
Fax: +390250314781;
Email: cinzia89.ferrario@alice.it, cinzia.ferrario@unimi.it

Manuscript received: March 12, 2015
Accepted in final form: June 17, 2015

DOI: 10.1111/wrr.12336

ABSTRACT

The red starfish *Echinaster sepositus* is an excellent model for studying arm regeneration processes following traumatic amputation. The initial repair phase was described in a previous paper in terms of the early cicatrisation phenomena, and tissue and cell involvement. In this work, we attempt to provide a further comprehensive description of the later regenerative stages in this species. Here, we present the results of a detailed microscopic and submicroscopic investigation of the long regenerative phase, which can be subdivided into two subphases: early and advanced regenerative phases. The early regenerative phase (1–6 weeks p.a.) is characterized by tissue rearrangement, morphogenetic processes and initial differentiation events (mainly neurogenesis and skeletogenesis). The advanced regenerative phase (after 6 weeks p.a.) is characterized by further differentiation processes (early myogenesis), and obvious morphogenesis and re-growth of the regenerate. As in other starfish, the regenerative process in *E. sepositus* is relatively slow in comparison with that of crinoids and many ophiuroids, which is usually interpreted as resulting mainly from size-related aspects and of the more conspicuous involvement of morphallactic processes. Light and electron microscopy analyses suggest that some of the amputated structures, such as muscles, are not able to replace their missing parts by directly re-growing them from the remaining tissues, whereas others tissues, such as the skeleton and the radial nerve cord, appear to undergo direct re-growth. The overall process is in agreement with the distalization-intercalation model proposed by Agata and co-workers. Further experiments are needed to confirm this hypothesis.

Regeneration has been described at both cellular and tissue levels in adult individuals of all echinoderm classes.[1–9] An important point concerning all postembryonic developmental processes, such as regeneration, is to understand the mechanisms allowing the cells of the developing structure to reform the ordered spatial pattern of differentiated tissues, at the correct place and at the right time, on the basis of positional information and morphogenetic gradients. According to Dubois and Ameye,[3] who studied starfish and sea urchin spine regeneration, during the regenerative events, the pattern of regrowth of missing parts depends on their total or partial removal: the regeneration of lost tissues is epimorphic, whereas the regenerative process of damaged tissues is morphallactic. It has been also documented that the process of regeneration changes according to the different tissue types. Dolmatov and Ginanova[10] showed that both the intestine and aquapharyngeal complex in holothurians follow a developmental pattern similar to that of asexual reproduction, whereas regeneration of muscles and tube feet follows the same pattern observed during their embryogenic development.

Asteroids are characterized by their ability to completely regenerate arms lost after amputation: for this reason they have been employed successfully as valuable experimental models for studies on regeneration exploring both morphological aspects (e.g., *Leptasterias hexactis* and *Asterias rubens*[1,2]) and molecular aspects (e.g., *Marthasterias glacialis*[11]). Similarly, *Echinaster sepositus* has been recently used as model species to investigate both microscopic anatomy[12] and molecular aspects (homeobox genes) of arm regeneration.[13]

ASW	Artificial sea water
CE	Coelomic epithelium
h p.a.	hour(s) postamputation
HMDS	Hexamethyldisilazane
RNC	Radial nerve cord
RWC	Radial water canal
SLSs	Spindle-like structures
SPAFG	Sucrose-picric acid-formaldehyde-glutaraldehyde
w p.a.	week(s) postamputation

As in most echinoderms, asteroid regenerative events include the following main steps: a *repair phase*, characterized by the first emergency reactions and the wound healing; an *early regenerative phase*, during which tissue reorganization and first signs of tissue regenerative phenomena occur; an *advanced regenerative phase*, characterized by restoration and tissue regrowth with the formation of a new small regenerating arm consisting of the same structures of the adult arm.[8,14]

In a previous work,[12] we studied the repair phase of *E. sepositus*, which lasts for one week after the traumatic amputation. This initial phase represents an important "preparation step" for the subsequent regenerative events involving the lost tissues. In the current work, we go further by providing a comprehensive and detailed analysis of the following regenerative phases, focusing on the tissue and cellular aspects of growth, morphogenesis and differentiation, which will represent an indispensable morphological complement to the molecular investigations.[13]

MATERIALS AND METHODS

Ethics statement

All animal manipulations were performed according to the Italian law, i.e. no specific permits were required for the described studies as starfish are invertebrates. *Echinaster sepositus* is not an endangered or protected species. All efforts were made to minimize the animal suffering during experimental procedures. The specimens were released into their natural environment once the experimental procedures were completed.

Animal sampling and regeneration tests

Adult (diameter ~12 cm) specimens of *Echinaster sepositus* were collected by scuba divers at depth of 5–8 m from the Marine Protected Area of Portofino (Paraggi, Ligurian Sea, Italy) between November 2012 and April 2013. They were left to acclimatize for two weeks and maintained at 18 °C in aerated aquaria filled with artificial sea-water (Instant Ocean, 37‰) for the whole experimental period. Chemical–physical sea water parameters were checked daily (temperature and salinity) or weekly (concentrations of nitrites, nitrates, Ca, Mg, PO_4, and pH) and promptly adjusted if necessary. Specimens were fed with small pieces of cuttlefish twice a week. Traumatic amputation of the distal third of one arm for each specimen was performed by scalpel. Animals were then left to regenerate in the aquaria for predetermined periods. The regeneration pattern was monitored at 1, 3, 6, 10, and 16 week(s) post-amputation (p.a.). Four-six samples/individuals were analyzed for each stage. Regenerating arm tissues were removed including about 1 cm of the stump and were subsequently processed for the different microscopic analyses.

Microscopic analyses

Regenerating tissues collected at different time points were analyzed by different microscopy techniques (light and electron, see below). Samples were initially observed and photographed under a LEICA MZ75 stereomicroscope provided with a Leica EC3 Camera and Leica Application Suite LAS EZ Software (Version 1.8.0).

Light microscopy

Both thick (paraffin) and semithin (resin) sections were prepared. Briefly, for thick sections three samples per stage were fixed in Bouin's fluid for about one month to allow decalcification, washed in tap water, dehydrated in an increasing ethanol series, cleared with xylene, washed in xylene:paraffin wax solution (1:1) and embedded in paraffin wax (56–58 °C). Sagittal (longitudinal-vertical) sections (5–7 μm) were cut and stained according to Milligan's trichrome technique. For resin sections, three samples per stage were fixed in SPAFG fixative (3% glutaraldehyde, 1% paraformaldehyde, 7.5% picric acid saturated solution, 0.45 M sucrose, 70 mM cacodylate buffer) for one month to allow decalcification, washed in 0.15 M cacodylate buffer and postfixed in 1% osmium tetroxide in the same buffer for 2 hours. Samples were rapidly washed in distilled water and then in 1% uranyl acetate in 25% ethanol (2 hours), dehydrated in an ethanol series, cleared in propylene oxide, washed in propylene oxide:Epon 812-Araldite solution (3:1 for 1 hour, 1:1 for 1 hour, 1:3 for 1 hour and 100% resin overnight) and embedded in Epon 812-Araldite. Samples were longitudinally sectioned using a Reichert Ultracut E with glass knives. The semithin (1 μm) sections were stained with crystal violet and basic fuchsin. Thick and semithin sections were observed under a Jenaval light microscope provided with a DeltaPix Invenio 3S 3M CMOS Camera and DeltaPix Viewer LE Software.

Scanning electron microscopy

The regenerating samples were fixed in scanning electron microscopy (SEM) A fixative (ASW 85% and glutaraldehyde 2%) for 2 hours at +4 °C and left in ASW overnight at the same temperature. Samples were post-fixed in SEM C fixative (ASW 36‰ with glucose 940 mOsM and osmium 2%) for 2 hours and subsequently washed with dH_2O to remove all traces of osmium. Afterwards, dehydration with an ethanol series was performed. Samples were transferred to a series of solutions of HMDS (Hexamethyldisilazane) in ethanol in different proportions (1:3, 1:1, 3:1, and 100% HMDS).

After sagittal sectioning, the remaining paraffin embedded half-samples were also used for SEM analyses. Samples were washed several times with xylene for 5 days to completely remove the paraffin wax. Then they were washed in absolute ethanol and subsequently in HMDS and ethanol (in the proportions: 1:3, 1:1, 3:1) for 15 minutes each wash, and then washed 3 times in 100% HMDS for 15 minutes each wash. Finally, all the processed samples were mounted on stubs, covered by a thin layer of pure gold (Sputter Coater Nanotech) and observed under a scanning electron microscope (LEO-1430).

Transmission electron microscopy

For transmission electron microscopy (TEM) analyses the same samples used for semithin sections were cut sagittally with glass knives using the same Reichert Ultracut E. The thin sections (0.07–0.1 μm) were collected on copper grids, stained with uranyl acetate followed by lead citrate

and finally carbon coated with an EMITECH K400X Carbon Coater. The thin sections were observed and photographed using a Jeol 100SX transmission electron microscope.

RESULTS

The regenerative phase was preceded by a repair phase lasting 72 hours, which was described in detail in a recent paper.[12] Here, we provide a brief description of the 72 hours p.a regenerating arm-tip morphology which represents the "background" to the subsequent regenerative events described in the present manuscript. At the end of the repair phase (72 hours p.a.), the arm-tip was completely closed over by a rather thick and differentiated epithelium, showing most of the typical cell types (including epidermal cells and underlying basiepithelial nervous plexus). Beneath this latter an initial accumulation of scattered heterogeneous cytotypes occurred: these were mainly phagocytes and dedifferentiating myocytes intermixed with new fibrils of collagen, overall forming an edematous area. The radial nerve cord (RNC) was similarly healed (Figure 1).[12]

Early regenerative phase

1 w p.a.: first sign of regrowth

One week after traumatic amputation, the newly formed epidermis was thick and well organized (Figures 2A and B). As already observed after 72 hours p.a.,[12] the supporting cells were elongated and partly differentiated, bearing microvilli and cilia. The connective tissue underlying the wound epidermis was relatively well developed. Cellular elements, including morphologically undifferentiated cells, phagocytes and dedifferentiated myocytes, increased in number in comparison to the previous stage and were intermixed with new collagen fibrils (72 h p.a.) (Figures 2C and 3A–D). In some cases, a single dedifferentiating contractile apparatus (SLS: "spindle-like" structure) was observed in phagosomes (Figures 3C and D). Large numbers of these different cell types appeared to migrate from the aboral and the oral body walls, the coelom, the nervous system and the tube feet towards the wound area (Figures 2D and E). All these changes resulted in the edematous area (see Figure 2) acquiring at one week both the structure and function of a fibrous cicatricial tissue (Figure 2E).

Seven days p.a. could be considered as a separate time point in the regenerative process from which the early processes of outgrowth and differentiation started, the main changes involving the coelomic canals, the RNC and the endoskeleton. Indeed, the perivisceral coelom with its newly formed mesothelial lining (CE) started regrowing after the complete fusion of the aboral and oral body wall edges. The somatic zone of the RNC also showed first signs of regeneration. The regenerating nerve portion was composed mainly of scattered and intermixed supporting cell elements. These latter were acquiring their typical bipolar shape, producing two opposite thin cytoplasmic extensions, in which regenerating intermediate filament bundles were already visible. These cell extensions produced a series of "niches," which started to be colonized by interspersed neurons (Figure 3E). The apical features of the neuroepithelium were not completely differentiated: in particular cilia, microvilli and cell junctions were not visible yet and the hyaline layer consisted only of a faint fuzzy material (Figure 3F).

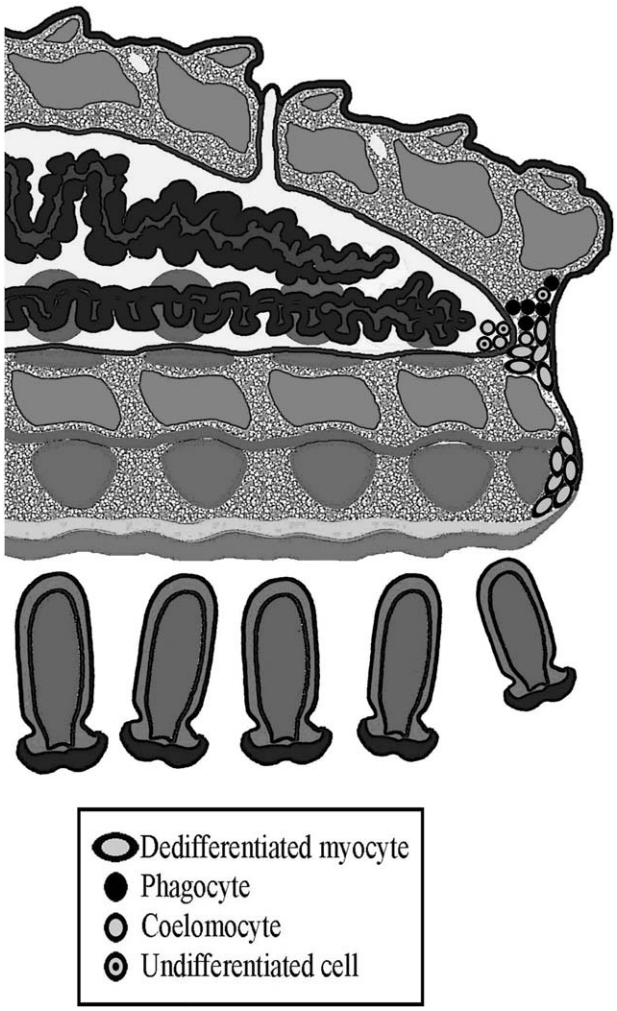

Figure 1. Diagram summarizing the main morphological characteristics of *E. sepositus* arm-tip at the end of the repair phase (72 h p.a.): Thick wound epithelium and edematous area formation: pool of various cells (myocytes, phagocytes, etc.) intermixed with newly deposited collagen fibrils.

At this same stage, the early signs of skeletogenesis were evident: initial mineral deposits of calcium carbonate in the form of primary plates could be detected within the new collagen network which was progressively forming in close bundles filling the former edematous area (Figure 2F).

3 w p.a.: the regenerate appearance

Three weeks after amputation a small regenerate appeared (~1.2 mm in length; Figures 4A and B). It was covered by an epidermis similar to that described above; although the inner stroma of connective tissue looked less compact and less organized in comparison with that of the stump, its

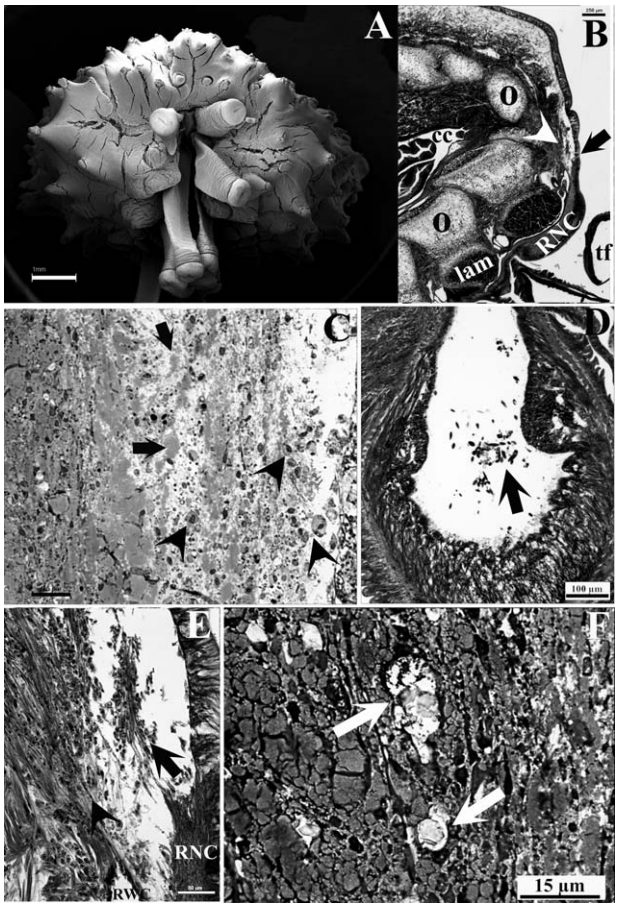

Figure 2. First sign of regrowth (1 w p.a.). (A) (SEM photo): A front view of the regenerating area showing the complete reepithelialisation of the injury. (B) (Light microscopy (LM)): The newly formed epidermis is thick and well organized (arrow) and the connective tissue underlying the wound epidermis is relatively well developed (arrowhead). (C) (LM): Cellular elements (arrowheads) found behind the wound epidermis intermixed with new collagen fibrils (arrows). (D) (LM): Dedifferentiating myocytes migrating from the stump tube foot towards the wound area (arrow). (E) (LM; a detail of B): The one week edematous area has a fibrous cicatricial tissue structure. Large numbers of different cell types appear to migrate from the water vascular system (RWC) (arrowhead) and the nervous system (RNC) (arrow). (F) (LM): Early signs of skeletogenesis: first mineral deposits of calcium carbonate in form of primary plates (arrows). cc, coelomic cavity; lam, longitudinal ambulacral muscle; o, ossicle; RNC, radial nerve cord; RWC, radial water canal; tf, tube foot.

collagen fibers appeared to be more oriented, forming a transverse meshwork. Inside the regenerate the developing ossicles were more differentiated. The mineralized part of the ossicles, the stereom, now formed a three dimensional meshwork of trabeculae. The radial water canal, which appeared to be more inflated, started regenerating the terminal tube foot (Figures 4C and D).

During this phase, tissues demonstrated an evident overlapping of both recycling and differentiation processes. In addition to the flow of cells to the growth area, the first

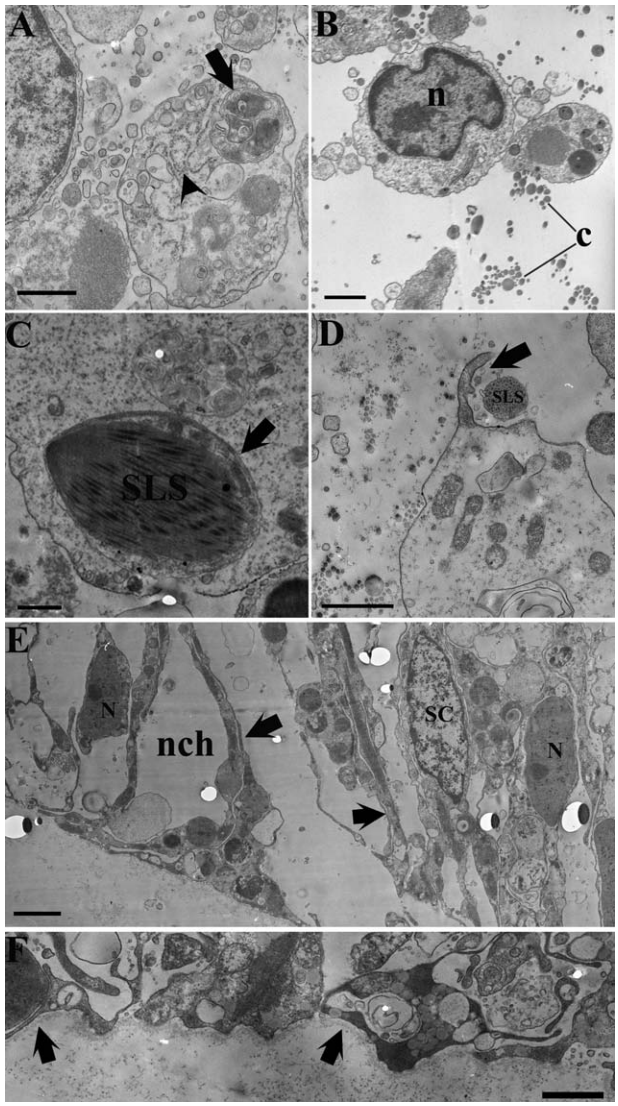

Figure 3. TEM micrographs of migrating cells and neurogenesis (1 w p.a.). (A) A phagocyte with obvious phagosome (arrow) and RER (arrowhead). (B) A presumptive undifferentiated cell with big nucleus (n) and widespread collagen fibrils (c). (C) Single dedifferentiating contractile apparatus (SLS) in phagosome (arrow). (D) Beginning of phagocytosis of a single dedifferentiating contractile apparatus by a phagocyte (arrow). (E) Regenerating nerve composed mainly of scattered supporting cell elements (SC) acquiring their typical bipolar shape in which regenerating intermediate filament bundles (arrows) are visible. "Niches" (nch) start to be colonized by interspersed neurons (N). (F) A faint fuzzy material (arrows) of the apical part of the neuroepithelium. c, collagen; n, nucleus; nch, niche; N, neuron; RER, Rough endoplasmic reticulum; SLS, spindle-like structure; SC, supporting cell. Scale bars: 1 µm (A, B, C, D, F); 2 µm (E).

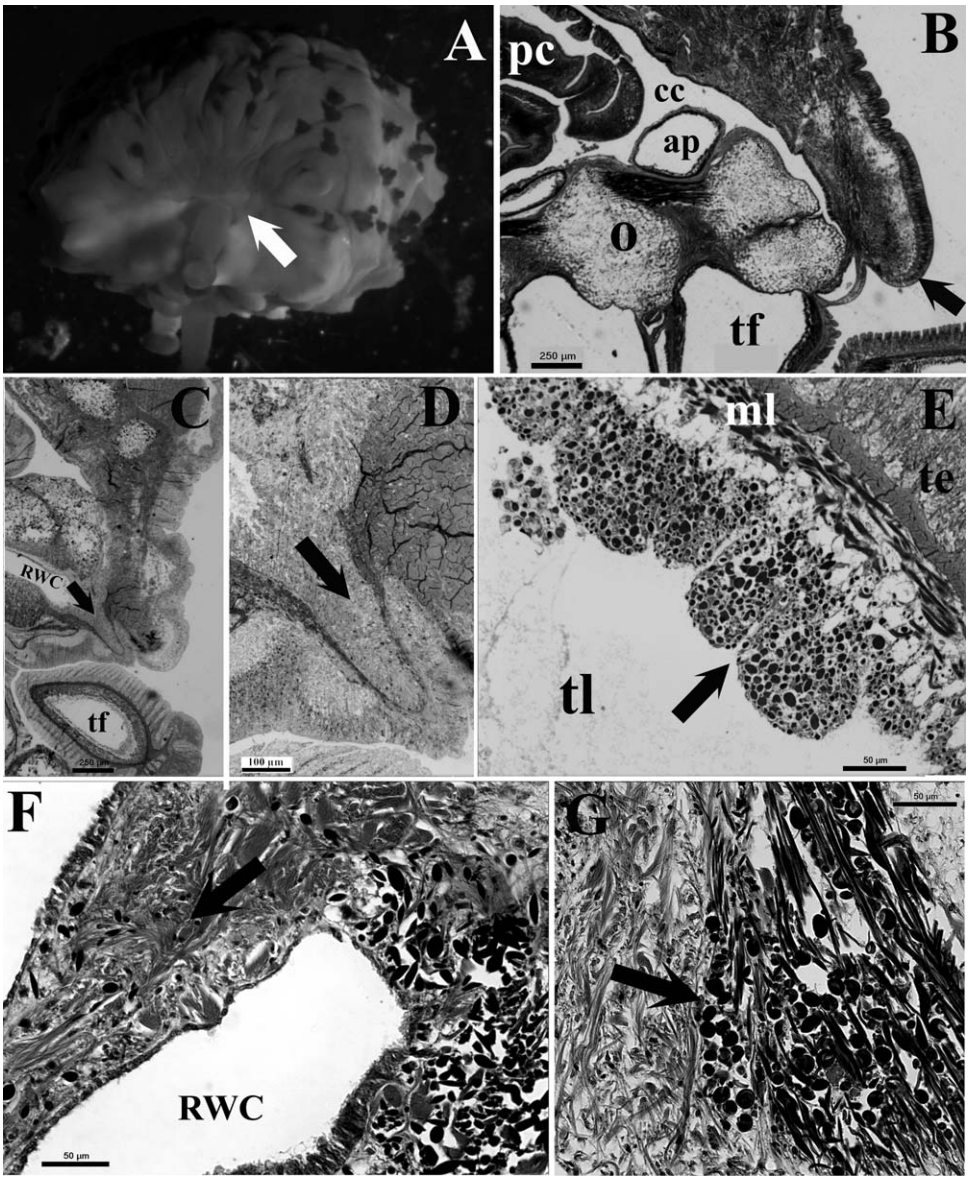

Figure 4. Appearance of the regenerate (3 w p.a.). (A) (stereomicroscopy (SM) view) and (B) (LM): A regenerate measuring about 1.2 mm in length (arrows). (C and D) (a detail of C) (LM): The radial water canal (RWC) regenerating the terminal tube foot (arrows). (E) (LM): Massive release of dedifferentiating myocytes from the inner coelomic wall to the lumen of the tube foot (arrow). (F) (LM): Flow of dedifferentiating myocytes to the growth area (arrow). (G) (LM): Uninjured muscle rearrangement (arrow). ap, ampulla; cc, coelomic cavity; ml, myoepithelial layer; o, ossicle; pc, pyloric caeca; RWC, radial water canal; te, tube foot epidermis; tf, tube foot; tl, tube foot lumen.

pair of tube feet showed a massive release of cells from their inner coelomic wall to the lumen (Figures 4E and F). Also the most distal uninjured muscle bundles displayed evident rearrangement processes (Figure 4G).

Advanced regenerative phase

6 w p.a.: myogenesis and tube feet morphogenesis

A new arm-tip measuring about 1.5 mm in length was clearly visible at 6 w p.a. (Figures 5A and B). New mucous glands were present in the form of invaginations of the epidermis (Figure 5C), under which small spines also started to develop. The stereom of the new skeletal structures (spines and ossicles) became more differentiated. The lateral processes from adjacent trabeculae tended to fuse together giving rise to the typical tridimensional meshwork of the stereom structure. TEM analyses at this skeletogenetic stage showed a number of cells of different types in the newly formed organic stroma: putative fibroblasts *(collagen-making cells)*, scleroblasts *(skeleton-making cells)* and phagocytes (Figure 6A). The *collagen-making cells* were distinguished by the presence of "multilamellar vesicles" in their cytoplasm and of two nucleoli in their nucleus (Figures 6A and B). Some of the presumptive phagocytes had a cilium at one pole (Figure 6C). The *skeleton-making cells* were distinguished by their cytoplasm containing a well developed and swollen Golgi complex, with associated vesicles, RER and other organelles. They were easily recognizable by their "calcification" vacuoles, at this stage containing only amorphous material, where calcite would be subsequently

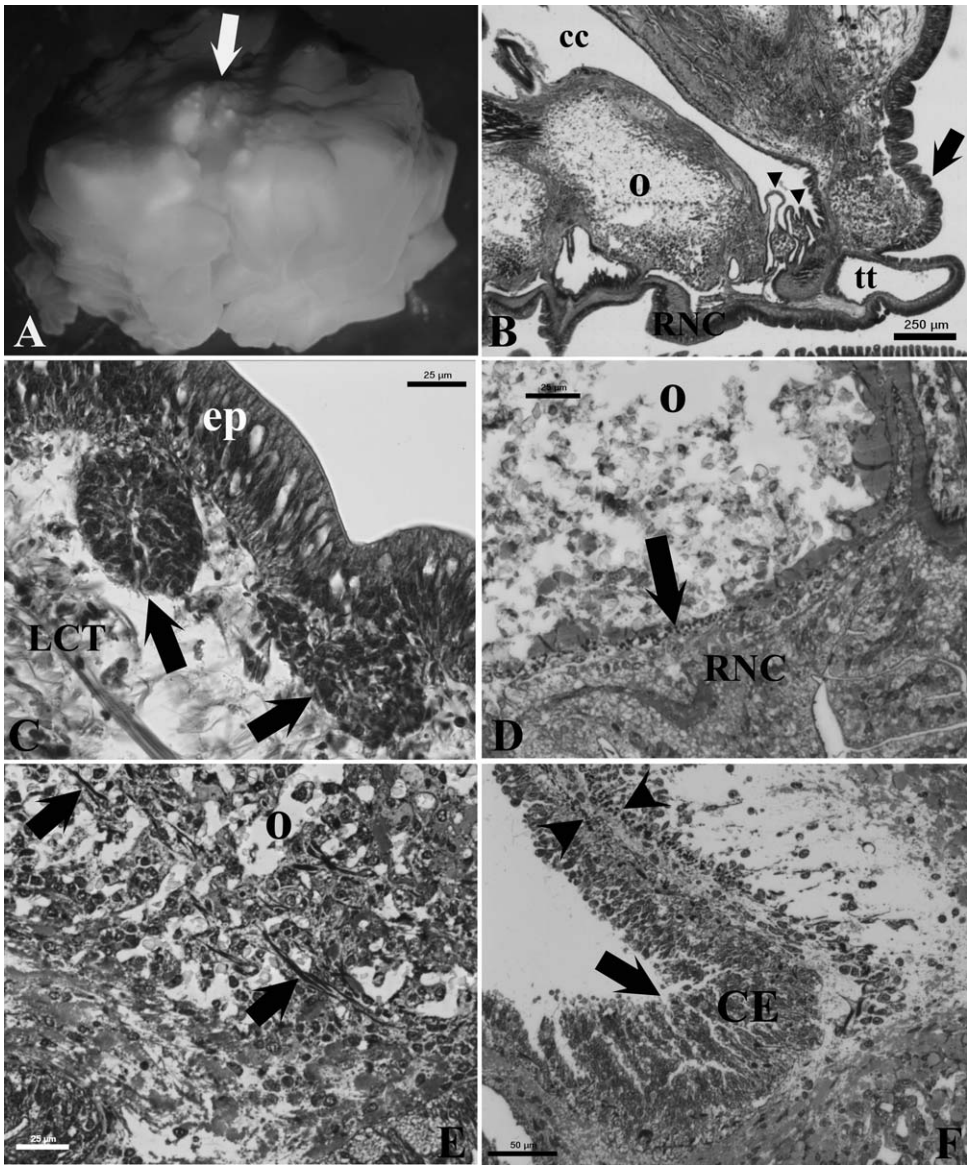

Figure 5. Myogenesis and tube foot morphogenesis (6 w p.a.). (A) (SM view) and (B) (LM): A clearly visible new arm-tip (arrows). The terminal tube foot (tt) is well developed. New tube feet (about four pairs) showing proximal-distal differentiation levels are visible in the regenerate (arrowheads). (C) (LM): New mucous glands forming as invaginations of the epidermis (arrows). (D) (LM): First signs of myogenesis related to the lower transverse ambulacral muscle (arrow). (E) (LM): Scattered myocytes detected among the developing ossicles (arrows). (F) (LM): The newly formed aboral CE is furrowed (arrow) and its longitudinal and circular muscles are regenerating progressively (arrowheads). cc, coelomic cavity; CE, coelomic epithelium; ep, epidermis; LCT, loose connective tissue; o, ossicle; RNC, radial nerve cord; tt, terminal tube foot.

deposited (Figures 6A, C, and D). In the regenerating ossicles the new collagen exhibited transverse and longitudinal bundles and contained developing spicules enveloped by several cell processes (Figure 6A).

First signs of myogenesis related to the lower transverse ambulacral muscles were clearly visible: they appeared as single transverse bundles of myocytes localized above the RNC (Figure 5D). Additionally, scattered myocytes could be detected among the developing ossicles (Figure 5E). Similarly, the longitudinal and circular muscles supporting the new CE were reorganizing and regenerating, although the overall architecture of this layer (especially the circular muscles) was still incomplete and far from being definitely organized. The myocytes composing this reforming circular layer apparently derived from the CE (Figure 5F). The regenerated epidermis and the newly formed aboral CE were furrowed.

The unpaired terminal tube foot was now well developed and protruded axially. The optic cushion started to differentiate the first pigment-cup ocelli. Six weeks p.a., new tube feet (about four pairs) were visible in the regenerate, showing proximal–distal differentiation levels (Figure 5B). The most proximal portion included small ampullae, in which an inner and an outer coelomic lining, separated by a middle layer of connective tissue, were easily recognizable.

10 w p.a.: complete restoration of the missing parts

At this time point the regenerating tip was about 1.7 mm in length (Figures 7A and B). The regenerative process was substantially completed: indeed, all the missing parts were restored, although still smaller in size (Figure 7B).

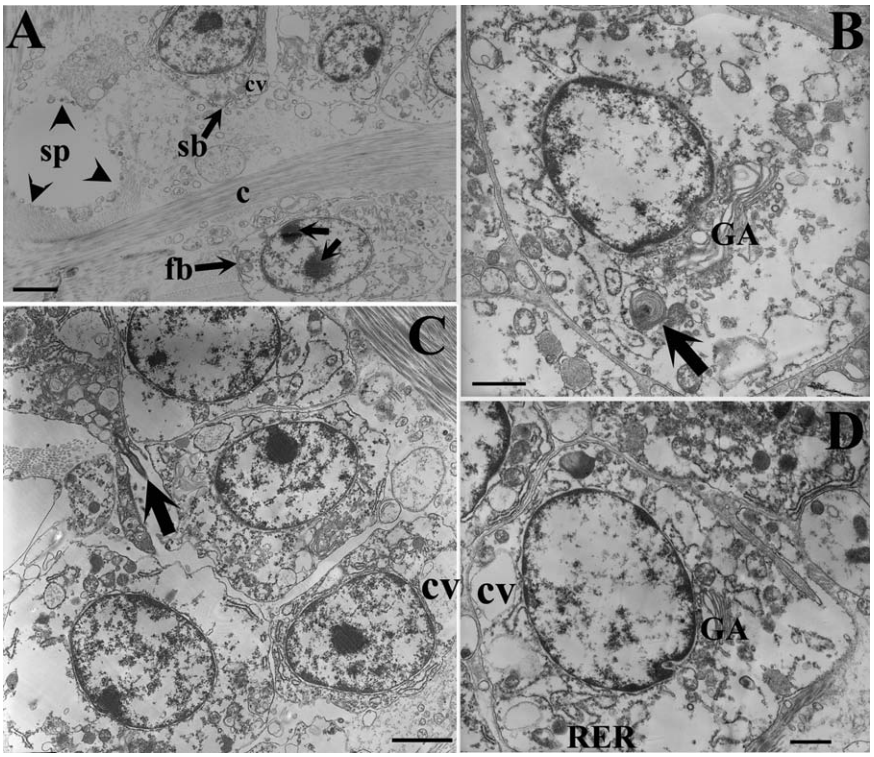

Figure 6. TEM micrographs of skeletogenesis (6 w p.a.). (A) A micrograph of the newly formed organic stroma showing putative fibroblast (fb) with two nucleoli (arrows) and scleroblast (sb) with calcification vacuole (CV), well organized new collagen (c) and developing spicule (sp) which are enveloped by several cell processes (arrowheads). (B) Detail of a collagen-making cell (fb) distinguished by the presence of "multilamellar vesicles" (arrow) and evident Golgi apparatus (GA) in its cytoplasm. (C) Presumptive phagocyte with a cilium at one pole (arrow) present in the newly formed stroma. (D) Detail of a skeleton-making cell (sb) which is easily recognizable by its cytoplasm containing calcification vacuoles (CV), GA and RER. c, collagen; CV, calcification vacuole; fb, fibroblast; GA, Golgi apparatus; RER, Rough endoplasmic reticulum; sb, scleroblast; sp, spicule. Scale bars: 1 μm (A, B, D); 2 μm (C).

The new aboral and oral ossicles and spines were well developed and organized (Figures 7B and C). The progressive development of the major muscle bundles continued, showing an increase in fiber number and size. In the TEM, each muscle bundle appeared to be composed of several tightly packed myocytes with large circular nuclei. In most cases the newly formed myofilaments were already well arranged in ordered contractile fields distributed in the peripheral regions of the fibers (Figure 7D). Developing muscles were not yet observed in the articulations between the new aboral ossicles. The tube feet (about six pairs), with well differentiated ampulla and podium components, still lacked terminal suckers (Figure 7B).

The newly regenerated segment of the radial nerve cord (RNC) gradually acquired all its components, namely a clearly recognizable optic cushion provided with several well differentiated pigment-cup ocelli (Figure 7E). The neural elements and the supporting cells of the regenerated part acquired their definitive shape and organization and became indistinguishable from those of the uninjured radial nerve.

A characteristic edematous area was visible just behind the folded distal CE (Figure 7B). This area contained different cell types (differentiating myocytes, nervous processes, and ciliated cells) intermixed with collagen fibrils (Figure 7F).

16 w p.a.: a minuscule arm

The new arm-tip, measuring about 3 mm in length, was well differentiated and actually resembled a miniature arm, showing all the typical features of the normal arm (Figures 8A and B). It had a terminal tube foot complete with a fully differentiated optic cushion. At least eight pairs of new tube feet were present, the most proximal pair showing developing suckers. Numerous dermal mucous glands and well differentiated spines were present. The upper transverse ambulacral muscles and the muscle bundles joining the aboral ossicles were also developed (Figure 8C). Although the pyloric caeca had healed, they did not extend into the coelomic cavity of the regenerate. No papulae were detectable at this stage of regeneration.

Rate of arm-tip regeneration

No arm-tip was visible at 1 w p.a.; the first sign of a measurable regenerate (about 1.2 mm in length) appeared after 3 weeks p.a. Arm growth was fast during the early regenerative phase (0.32 mm/week), then it decreased regularly in the advanced regenerative phase (0.13 mm/week). The overall rate of arm-tip regeneration was about 0.2 mm/week. The lost arm could be replaced completely in about two or three years in captivity (personal observations).

To standardize for size/age effect, the measured lengths (mm) of the regenerating arms (starting from the amputation plane) were expressed as a proportion of the corresponding diameters (mm) of arm stumps measured from the top (aboral) to the base (oral), at about 1 cm far from the amputation plane of each arm, excluding the tube foot length. The normalized values are plotted against time in Figure 9. A logarithmic curve was the best model to describe the relationship ($R^2 = 0.9796$).

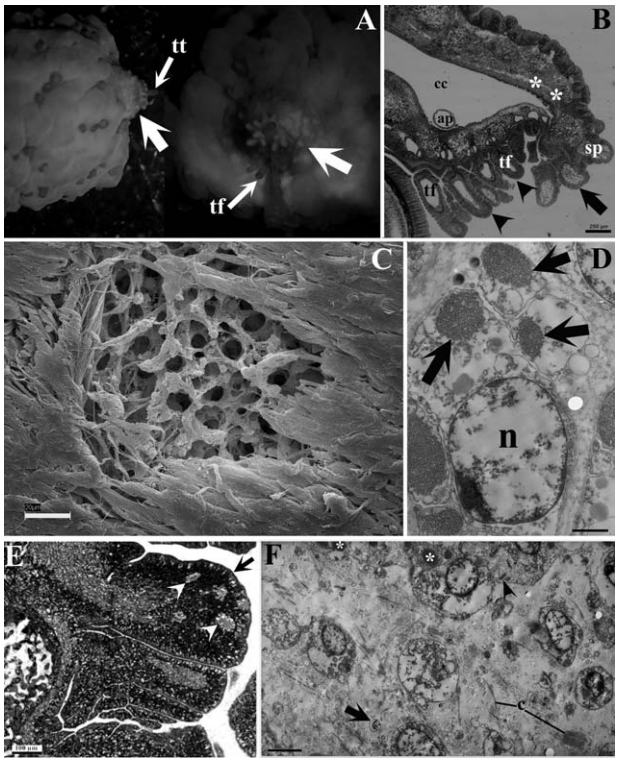

Figure 7. Complete restoration of the missing parts (10 w p.a.). (A) (SM view): A top view (left) and a front view (right) of the regenerate (arrows) showing the terminal tube foot (tt) and new tube feet (tf). (B) (LM): Restoration of all the missing parts. Spines are well developed (arrow). The tube feet are well differentiated, but still lack final suckers (arrowheads). An edematous area is visible just behind the folded distal CE (asterisks). (C) (SEM micrograph): A well developed and organized new ossicle. (D) (TEM micrograph): New myocytes with large circular nuclei (n) and newly formed myofilaments (arrows). (E) (LM): A clearly recognizable optic cushion (arrow) provided with several well differentiated pigment-cup ocelli (arrowheads). (F) (TEM micrograph): A detail of the edematous area just behind the folded distal CE: different cell types (differentiating myocytes (asterisks), nervous processes (arrow), and ciliated cells (arrowhead)) are intermixed with collagen fibrils (c). ap, ampulla; c, collagen; cc, coelomic cavity; CE, coelomic epithelium; n, nucleus; sp, spine; tf, tube foot; tt, terminal tube foot; *, oedematous area (B), differentiating myocytes (F). Scale bars: 1 μm (D); 4 μm (F).

DISCUSSION

Regenerative phase

The regenerative phase is the core of the regeneration process and, due to its complexity and duration, can be subdivided into early and advanced subphases. During the early subphase, the connective tissue develops at the wound site and the first calcitic skeletal deposits are observed. The edematous area is still evident at this stage, possibly playing a "structural" role related to the defensive function typical of the repair phase.[12] Obvious cell migrations

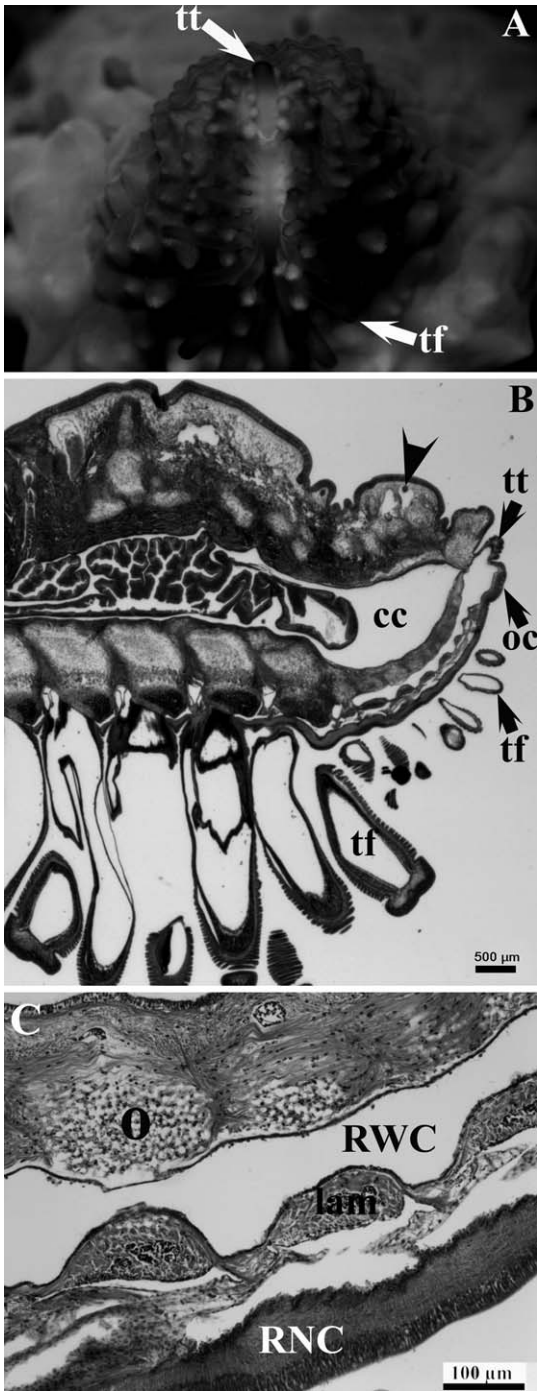

Figure 8. Regenerating arm (16 w p.a.). A (SM view): (A) front view of the regenerate measuring about 3 mm in length with complete terminal tube foot (tt) and at least six pairs of new tube feet (tf). (B) (LM): Regenerate with a complete terminal tube foot (tt) and a fully differentiated optic cushion (oc). Mucous glands (arrowhead) are well differentiated. (C) (LM): The lower transverse ambulacral muscles are well developed. cc, coelomic cavity; lam, lower ambulacral muscle; o, ossicle; oc, optic cushion; RNC, radial nerve cord; RWC, radial water canal; tf, tube foot; tt, terminal tube foot.

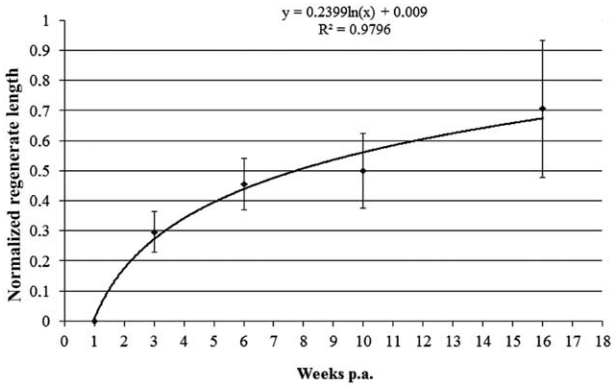

Figure 9. Time course of arm regeneration in *E. sepositus*. The regenerate length is expressed as a proportion of the stump diameter. N (number of samples for each time point) = 4. Bar = mean ± SD.

involving different cytotypes, are directed to this region where the regeneration of the new tissues eventually takes place. The 1 w p.a. edematous area is therefore an active "growth area." This is in agreement with observations of Mladenov and co-workers[1] who suggested that (1) the new structures are formed between the wound epidermis and the stump (in the growth area) and (2) the radial water canal and the radial nerve cord (the only two continuous structures along the arm) are restored by outgrowth from the remains of these structures in the stump. According to Dubois and Ameye[3] this second mechanism is similar to the developmental process during asexual reproduction which requires remaining parts of the tissues (stump); conversely the ex novo restoration of the lost structures, such as ossicles, muscles and tube feet, may resemble their developmental processes during embryogenesis.

Skeletogenesis

In *E. sepositus*, regeneration of lost skeletal ossicles can be divided into two stages, the first (1 w p.a.) characterized by initial mineral deposits and the second characterized by stereom meshwork formation and growth. At 6w p.a. TEM analyses have revealed that new ossicle formation in this starfish occurs in a manner similar to the sea urchin larval spicule[15] and primary tooth plate formation[16] and to spicule formation in holothurians.[17] As described in these models, skeleton formation begins with the aggregation of a population of more or less differentiated cells, including sclerocytes: these latter have one or more vacuoles where organic matrix is deposited. This initially intracellular spicule formation becomes then extracellular while the calcite crystal grows. In *A. rubens* Dubois and Jangoux[18] reported that spicule formation might be initiated both intracellularly (lost skeleton) or extracellularly (damaged skeleton).

TEM examination at the level of the stroma in 6 w p.a. regenerating ossicles revealed the presence of many fibrocytes close to scleroblasts. These cells produce collagen, glycosaminoglycans and other glycoproteins usually found in the extracellular matrix. It has been demonstrated that some of these extracellular components are fundamental for normal spicule formation. Spicule development may be inhibited if the extracellular matrix lacks N-linked glycoproteins[19] and inhibition of collagen formation prevents normal spicule growth.[20,21] Hence, in addition to their role in stroma collagen formation, fibroblasts found in *E. sepositus* might be also involved in stereom construction.

The presence in the developing stereom of monociliated phagocytes is quite unusual, although previously described in *A. rubens* by Dubois and Ameye.[3] This feature further supports the hypothesis that phagocytes may derive from or share a common origin with coelomocytes.

Myogenesis

Two different coexisting events have been observed in *E. sepositus* muscular tissues following arm amputation: dedifferentiation and differentiation. The former includes different mechanisms depending on the integrity of the muscular tissue. Standard tissue histolysis is observed at the level of injured muscles from the very first stages of the repair phase.[12] A different mechanism occurs at the level of some intact muscle bundles far from the amputation site (such as the lower transverse ambulacral muscle or the myocytes composing the tube foot wall) and can be regarded as an "induced dedifferentiation." This process becomes particularly active at 3 w p.a. in parallel with the remarkable growth of the regenerate. This observation supports the idea that these dedifferentiated myocytes, once reprogrammed, actively contribute to histogenesis and organogenesis of the regenerating structures.[22]

During myogenesis it is suggested that at the regeneration site some of the CE cells ingress, then they detach from the overlying epithelium and acquire the myocyte phenotype.[9,10] This hypothesis is in agreement with what we observed in *E. sepositus* at 6 w p.a., where the longitudinal muscle layer of the stump CE apparently penetrates deeply into the underlying connective tissue of the regenerate giving rise to the new circular muscle layer. Similarly, during the regeneration of the somatic muscle of two holothurians (*Eupentacta fraudatrix* and *Apostichopus japonicus)* the basal regions of the coelomic epithelium detach from the surface epithelium to close up and form elongated tubular structures that eventually become new muscle bundles.[23,24]

Moreover, it has been documented that myocytes do not undergo cell division once they have acquired their typical differentiated form.[9] According to the authors, each newly formed myocyte is derived from a new cell from the CE, which retains the capacity to divide. This might explain the inability of *E. sepositus* to repair damaged muscles, which therefore necessitates the recycling and reformation of whole muscles.

However, there is no definitive evidence demonstrating that the origin of new myocytes is restricted only to CE elements. Dedifferentiated myocytes might also contribute directly to the development of new muscles as previously suggested for crinoids.[22]

Turnover zone

After 6–10 weeks p.a. the CE at the level of the regenerating tip appears highly folded. In the underlying loose connective tissue a pool of scattered cells of various types is visible, including differentiating myocytes and phagocytes. Some of these cells might originate from the CE, as

suggested for phagocytes, fibroblasts[25] and myocytes.[9] However, it cannot be excluded that this is a grouping zone of migratory cells coming from distant origins. Indeed, Hernroth and co-workers[8] demonstrated that many cells are derived from distant tissues during arm regeneration in *A. rubens*, for example, from the pyloric caeca.

Neurogenesis

Regeneration success in starfish depends on the presence of neurotrophic substances released by the nervous system, which acts as the primary source of regulatory factors, mitogens or morphogens.[2,26–29] In *E. sepositus* within 72 h p.a. the subepidermal nerve plexus is completely regenerated,[12] whereas the RNC requires a slightly longer time: after a week p.a. the network of supporting cells with scattered neurons is visible. It has been demonstrated that neuron regeneration is guided by the radial glia cells which represent the main source of new cells in the regenerating radial nerve cord of echinoderms.[30] However, questions concerning the specific mechanisms of regrowth, such as the involvement of stem cells, dedifferentiation of local tissues or transdifferentiation in the regenerating nerve have not been fully investigated, especially in asteroids. There is some evidence suggesting that neurons in *A. rubens* are derived from locally dividing cells, but it cannot be confirmed whether neurons are derived from proliferation or transdifferentiation of neuroepithelial cells, although the former mechanism is suggested.[2] In our study it was difficult to detect the origin of new neurons in the radial nerve from histological analyses alone.

Rate of arm-tip regeneration

As in other starfish, such as *A. rubens* and *L. hexactis*,[1,2] the regeneration process in *E. sepositus* is very slow in comparison with that of crinoids[4] and some ophiuroids[8]: a tiny outgrowing regenerate appears only three weeks after traumatic amputation, whereas this can be seen after only 3 days in *A. mediterranea*[22] or after 4 days in *A. filiformis*.[8] Nevertheless, *E. sepositus* growth rate is slightly higher than that of some other larger ophiuroid species such as *Ophioderma longicaudum* (0.2 vs. 0.17 mm/week, respectively[8]). The marked differences from the crinoid *A. mediterranea* and the ophiuroid *A. filiformis* are often related to the prominent role of morphallactic processes during asteroid arm regeneration and to specimen size/age.[31] Nevertheless, this is not always true as pointed out by Biressi and co-workers[8] for ophiuroids. This concept appears valid also for asteroids in the present study: the regenerate appearence observed in *E. sepositus* (3 weeks) is comparable to that of smaller starfish like *L. hexactis*.[1] Overall there is apparently an arm size threshold which affects growth rate: below this limit regeneration occurs very rapidly, whereas above it there is a high interspecific variability. To avoid the effect of these factors, we chose *E. sepositus* adult specimens of similar size and we expressed the regenerate length as the ratio between its actual length and stump diameter. The use of this approach will certainly make easier future interspecific comparison.

Environmental variables, such as food and physical factors that is, salinity,[32] temperature and pH, can affect the regeneration rate.[33,34] Nevertheless, these factors are not relevant to our experimental tests. Temperature, pH and salinity were regularly monitored and maintained constant, no hypoxia was detected and the food quality was never changed during the experimental period: all the starfish experienced the same experimental conditions.

Additionally, we noticed that specimens of *E. sepositus* apparently require little, if any, nourishment during the first two weeks of regeneration of their missing parts. The same observation has been reported for the starfish *Asterias vulgaris*[35] and *Heliaster helianthus*[36]: after the loss of the arm animals apparently allocate energy to the process of arm regeneration rather than to feeding activity.

Regenerative process in *E. sepositus* in relation to the old and new concepts of regeneration

According to the classic definitions and concepts, regeneration can be classified as epimorphic or morphallactic depending on whether or not a localized blastema of proliferating progenitor cells is formed after wound healing.[37] A further distinctive element to be considered is the origin of cells involved in regeneration: are they undifferentiated or dedifferentiated/transdifferentiated elements? However, recent evidence indicated that these two mechanisms largely overlap and that in many cases both contribute to the overall regenerative process.[4,5]

According to classic principles the regeneration process of *E. sepositus* would be regarded as being mainly morphallactic because no distinct blastema is evident, even though a population of presumptive undifferentiated cells can be observed throughout the developing connective tissue below the wound epidermis. In agreement with our results, regeneration studies on various echinoderms report an initial accumulation, but not a proliferation, of coelomocytes beneath the wound epidermis[1,2] and suggest that migrating coelomocytes are recruited for wound healing.[4,38] In addition, the rearrangement of injured muscles immediately after amputation is considered a further characteristic morphallactic event. However, the old definitions of regenerative mechanisms are no longer adequate in the light of the present knowledge. Even one of the most studied models—planarian regeneration, has been described alternatively as an example of morphallaxis or epimorphosis.[37] According to Agata and co-workers,[39] in this model the blastema is formed as a signalling center to reorganize body regionality rather than a place of reforming lost tissues and organs; therefore they suggested the "distalization-intercalation" model as a general principle for vertebrates and invertebrates' regeneration. As the name indicates, according to this model organisms initially form the most distal part (distalization) of the new structure, which, by interacting with the underlying old stump tissues, induces reorganization of positional information. The lost structures are then recovered by appropriate intercalation of newly generated tissues between the distal part and the stump. As in all cases of asteroid arm regeneration, the terminal tube foot of *E. sepositus* (and partially the terminal ossicle) can be considered as the most distal elements (distalization) which drive the following intercalation process: indeed, the new structures such as tube feet, muscle bundles, and so forth gradually develop between the stump and the terminal structures with a proximal–distal gradient. In those starfish species where the terminal ossicle is naturally more developed (e.g.,

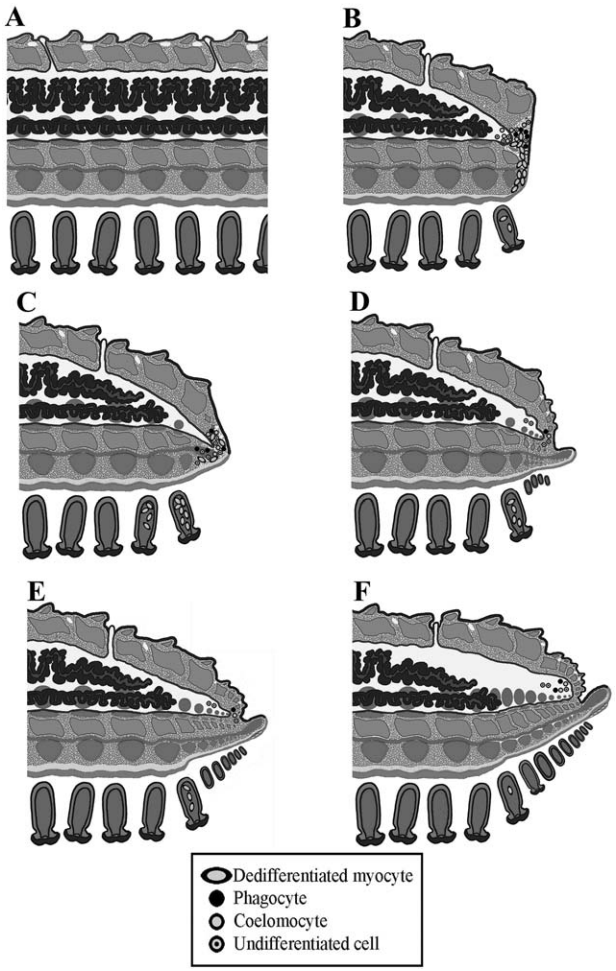

Figure 10. Diagram summarizing the main events during the regenerative phase of *E. sepositus*. (A) Gross morphology of non regenerating arm. (B) First sign of re-growth (1 w p.a.): cellular elements found behind the wound epidermis intermixed with new collagen fibrils and first sign of skeletogenesis. (C) The regenerate appearance (3 w p.a.): massive release of dedifferentiating myocytes from their inner coelomic wall to the lumen of the tube feet. (D) Myogenesis and tube feet morphogenesis (6 w p.a.): a clearly visible new arm-tip. The terminal tube foot is well developed. (E) Complete restoration of the missing parts (10 w p.a.). (F) A minuscule arm (16 w p.a.).

Marthasterias glacialis) its contribution as a distalization element is more clearly observable (personal observation). Other authors suggested that the concepts of distalization and intercalation are also applicable to arm regeneration in the starfish *Linckia laevigata* and *A. rubens*[40] and in the feather star *Oxycomanthus japonicus*.[41] In the crinoid *Antedon mediterranea* the most distal part of a normal arm maintains always the characteristics of an undifferentiated bud[22]: so during arm regeneration, even if a clearly recognizable and differentiated distal element is apparently not present, the blastema could be regarded as the true distal element.

These concepts simplify the controversial issue regarding the presence/absence of a blastema as the distinctive character of epimorphic/morphallactic mechanism. However, this does not solve the more persistent question related to the origin of cells involved in regeneration processes. In our opinion, the regenerative event should be classified *only according* to the origin of the cells recruited in regenerative process, which can be stem cells, dedifferentiated cells or both. In *E. sepositus* the presence of dedifferentiated elements (myocytes) might indicate the involvement of a morphallactic mechanism, but recently Hernroth and co-workers[6] demonstrated the involvement also of progenitor undifferentiated cells in the arm regeneration of *A. rubens*.

CONCLUSION

The overall process of arm regeneration in *E. sepositus* can be subdivided into three main phases: a first *Repair* phase (0–7 days), characterized by wound healing and edematous area formation; a second *Early regenerative* phase (1–6 weeks p.a.), during which the first sign of neo-formation of lost parts appears; and a third *Advanced regenerative* phase (from 6 w p.a.), characterized by a progressive development of the regenerating arm-tip. Figure 10 schematically summarizes the main processes occurring after the repair phase. During the regenerative phase a spatial and chronological differentiation of lost and injured structures occurs, starting from neurogenesis, skeletogenesis and water vascular system (terminal tube foot) development. Later, when the regenerate is clearly evident, myogenesis takes place between the newly formed skeletal ossicles and the tube feet start differentiating. The overall process is in agreement with the distalization–intercalation model proposed by Agata and co-workers.[37]

Future studies should investigate the regenerative process of each new structure using immunohistochemical and molecular tools to clarify the origin of the cells contributing to their regrowth.

ACKNOWLEDGMENTS

This research was founded by Young Researcher Grant (University of Milan, PI: Dr. M. Sugni). We would like to deeply thank the CIMA Center (Centro Interdipartimentale Microscopia Avanzata, University of Milan) for technical support in electron microscopy analyses. We are grateful to the Marine Protected Area of Portofino (Ligurian Sea, Italy) for permission to collect experimental animals and to the scuba divers Dario Fassini and Livio Leggio for the collection.

Conflict of interest disclosure: The Authors certify that there is no conflict of interest with any financial organization regarding the material discussed in the manuscript.

REFERENCES

1. Mladenov PV, Bisgrove B, Aostra S, Burke RD. Mechanisms of arm-tip regeneration in the sea star *Leptasterias hexactis*. *Roux Arch Dev Biol* 1989; 198: 19–28.
2. Moss C, Hunter J, Thorndyke MC. Pattern of bromodeoxyuridine incorporation and neuropeptide immunoreactivity during arm regeneration in the starfish *Asterias rubens*. *Phil Trans R Soc Lond B* 1998; 353: 421–36.

3. Dubois P, Ameye L. Regeneration of Spines and Pedicellariae in Echinoderms. A Review. *Microsc Res Tech* 2001; 55: 427–37.
4. Candia Carnevali MD. Regeneration in echinoderms: repair, regrowth, cloning. *ISJ* 2006; 3: 64–76.
5. Candia Carnevali MD, Burighel P. *Regeneration in echinoderms and ascidians*. ELS. Wiley: Chichester, 2010.
6. Hernroth B, Farahani F, Brunborg G, Dupont S, Dejmek A, Sköld H. Possibility of mixed progenitor cells in sea star arm regeneration. *J Exp Zool (Mol Dev Evol)* 2010; 6: 457–68.
7. Gorshkov AN, Blinova MI, Pinaev GP. Ultrastructure of Coelomic Epithelium and Coelomocytes of the Starfish *Asterias rubens* L. in Norm and after Wounding. *Cell Tissue Res* 2009; 3: 477–90.
8. Biressi A, Ting Z, Dupont S, Dahlberg C, Di Benedetto C, Bonasoro F et al. Wound-healing and arm regeneration in *Ophioderma longicaudum* and *Amphiura filiformis* (Ophiuroidea, Echinodermata): Comparative morphogenesis and histogenesis. *Zoomorphology* 2010; 129: 1–19.
9. García-Arrarás JE, Dolmatov IY. Echinoderms; potential model systems for studies on muscle regeneration. *Curr Pharm Des* 2010; 16: 942–55.
10. Dolmatov IY and Ginanova TT. Muscle regeneration in holothurians. *Microsc Res Tech* 2001; 55: 452–63.
11. Franco C, Soares R, Pires E, Kocil K, Almeida AM, Santos R et al. Understanding regeneration through proteomics. *Proteomics* 2013; 13: 686–709.
12. Ben Khadra Y, Ferrario C, Di Benedetto C, Said K, Bonasoro F, Candia Carnevali MD et al. Wound repair during arm regeneration in the red starfish *Echinaster sepositus*. *Wound Repair Regen* 2015, In press, DOI:10.1111/wrr.12333.
13. Ben Khadra Y, Said K, Thorndyke M, Martinez P. Homeobox Genes Expressed During Echinoderm Arm Regeneration. *Biochem Genet* 2014; 52: 166–80.
14. Candia Carnevali MD, Bonasoro F, Welsch U, Thorndyke MC. Arm regeneration and growth factors in crinoids. In: Mooi R, Telford M, editors. *Echinoderms*. San Francisco Rotterdam: Balkema 1998; 145–150.
15. Okazaki K. Skeleton formation of sea urchin larvae. II. Organic matrix of the spicule. *Embryologia* 1960; 5: 283–320.
16. Chen CP, Lawrence JM. The Ultrastructure of the Plumula of the Tooth of *Lytechinus variegatus* (Echinodermata: Echinoidea). *Acta Zool* 1986; 67: 33–41.
17. Sticker SA. The ultrastructure and formation of the calcareous ossicles in the body wall of the sea cucumber *Leptosynapta clarki* (Echinodermata, Holothuroida). *Zoomorphology* 1985; 105: 209–22.
18. Dubois Ph, Jangoux M. Stereom morphogenesis and differentiation during regeneration of fractured adambulacral spines of *Asterias rubens* (Echinodermata, Asteroidea). *Zoomorphology* 1990; 109: 263–72.
19. Grant WT, Sussman MD, Balian G. A disulfide-bonded short chain collagen synthesized by degenerative and calcifying zones of bovine growth plate cartilage. *J Biol Chem* 1985; 260: 3798–803.
20. Mintz GR, Lennarz WJ. Spicule formation by cultured embryonic cells from the sea urchin. *Cell Diff* 1982; 11: 331–333.
21. Blankenship J, Benson S. Collagen metabolism and spicule formation in sea urchin micromeres. *Exp Cell Res* 1984; 152: 98–104.
22. Candia Carnevali MD, Bonasoro F. Microscopic overview of crinoid regeneration. *Microsc Res Techniq* 2001; 55: 403–26.
23. Dolmatov IY, Eliseikina MG, Ginanova TT. Muscle repair in the holothurians *Eupentacta fraudatrix* is realized at the expense of transdifferentiation of the coelomic epithelium cells. *Biol Bull* 1995; 22: 490–5.
24. Dolmatov IY, Eliseikina MG, Bulgakov AA, Ginanova TT, Lamash NE, Korchagin VP. Muscle regeneration in the holothurian *Stichopus japonicus*. *Roux's Arch Dev Biol* 1996; 205: 486–93.
25. Dubois Ph, Ghyoot M. Integumentary resorption and collagen synthesis during regression of headless pedicellariae in *Sphaerechinus granularis* (Echinodermata: Echinoidea). *Cell Tissue Res* 1995; 282: 297–309.
26. Huet M. Le rôle du système nerveux au cours de la régénération du bras chez une étoile de mer: *Asterina gibbosa*. *J Embryol Exp Morph* 1975; 33: 535–52.
27. Huet M, Franquinet R. Histofluorescence study and biochemical assay of catecholamines (Dopamine and Noradrenaline) during the course of arm-tip regeneration in the starfish, *Asterina gibbosa* (Echinodermata, Asteroidea). *Histochemistry* 1981; 72: 149–54.
28. Thorndyke MC, Candia Carnevali MD. Regeneration neurohormones and growth factors in echinoderms. *Can J Zool* 2001; 79: 1171–208.
29. Thorndyke MC, Chen WC, Beesley PW, Patruno M. Molecular approach to echinoderm regeneration. *Microsc Res Tech* 2001; 55: 474–85.
30. Mashanov VS, Zueva OR, García-Arrarás JE. Radial glial cells play a key role in echinoderm neural regeneration. *BMC Biol* 2013; 11: 49.
31. Lawrence JM. Arm loss and regeneration in Asteroids (Echinodermata). In: Scalera-Liaci L, Canicatti C, editors. *Echinoderm research 1991*, Balkema: Rottardam; 1992.
32. Kaack KE, Pomory CM. Salinity effects on arm regeneration in *Luidia clathrata* (Echinodermata: Asteroidea). *Mar Freshw Behavi Phy* 2011; 44: 359–74.
33. Schram JB, McClintock JB, Angus RA, Lawrence JM. Regenerative capacity and biochemical composition of the sea star *Luidia clathrata* (Say) (Echinodermata: Asteroidea) under conditions of near-future ocean acidification. *J Exp Mar Biol Ecol* 2011; 407: 266–74.
34. Clark MS, Souster T. Slow arm regeneration in the Antarctic brittle star *Ophiura crassa* (Echinodermata, Ophiuroidea). *Aquatic Biol* 2012; 16: 105–13.
35. King HD. Regeneration in *Asterias vulgaris*. *Wilhelm Roux Arch Entwicklungsmech Org* 1898; 17: 351–63.
36. Barrios JV, Gaymer CF, Vasquez JA, Brokordt KB. Effect of the degree of autotomy on feeding, growth, and reproductive capacity in the multi-armed sea star *Heliaster helianthus*. *J Exp Mar Biol Ecol* 2008; 361: 21–7.
37. Agata K, Saito Y, Nakajima E. Unifying principles of regeneration I: Epimorphosis versus morphallaxis. *Dev Growth Differ* 2007; 49: 73–8.
38. Candia Carnevali MD, Thorndyke MC, Matranga V. Regenerating echinoderms; a promise to understand stem cells potential. In: Rinkevich B, Matranga V, editors. *Stem cells in marine organisms*. Heidelberg: Springer, 2009: 165–86.
39. Agata K, Tanaka T, Kobayash C, Kato K, Saitoh Y. Intercalary regeneration in planarians. *Dev Dyn* 2003; 226: 308–16.
40. Hotchkiss FHC. Arm stumps and regeneration models in Asteroidea (Echinodermata). *Proc Biol Soc Wash* 2009; 122: 342–54.
41. Shibata TF, Oji T, Akasaka K, Agata K. Staging of regeneration process of an arm of the feather star *Oxycomanthus japonicus* focusing on the oral-aboral boundary. *Dev Dyn* 2010; 239: 2947–61.